ELSEVIER

Biophysical Chemistry 125 (2007) 117–126

Biophysical Chemistry

http://www.elsevier.com/locate/biophyschem

The β-turn scaffold of tripeptide containing an azaphenylalanine residue

Ho-Jin Lee, Hyun-Mee Park, Kang-Bong Lee *

Advanced Analysis Center, Korea Institute of Science and Technology, P.O. Box 131 Cheongryangri, Seoul 130-650, Korea

Received 27 September 2005; received in revised form 10 May 2006; accepted 10 May 2006
Available online 4 August 2006

Abstract

The conformational preferences of azaphenylalanine-containing peptide were investigated using a model compound, Ac-azaPhe-NHMe with *ab initio* method at the HF/3-21G and HF/6-31G* levels, and the seven minimum energy conformations with *trans* orientation of acetyl group and the 4 minimum energy conformations with *cis* orientation of acetyl group were found at the HF/6-31G* level if their mirror images were not considered. An average backbone dihedral angle of the 11 minimum energy conformations is $\phi = \pm 91° \pm 24°$, $\psi = \pm 18° \pm 10°$ (or $\pm 169° \pm 8°$), corresponding to the $i+2$ position of β-turn (δ_R) or polyproline II (β_P) structure, respectively. The χ_1 angle in the aromatic side chain of azaPhe residue adopts preferentially between ±60° and ±130°, which reflect a steric hindrance between the N-terminal carbonyl group or the C-terminal amide group and the aromatic side chain with respect to the configuration of the acetyl group. These conformational preferences of Ac-azaPhe-NHMe predicted theoretically were compared with those of For-Phe-NHMe to characterize the structural role of azaPhe residue.

Four tripeptides containing azaPhe residue, Boc-Xaa-azaPhe-Ala-OMe [Xaa = Gly(**1**), Ala(**2**), Phe(**3**), Asn(**4**)] were designed and synthesized to verify whether the backbone torsion angles of azaPhe reside are still the same as compared with theoretical conformations and how the preceding amino acids of azaPhe residue perturb the β-turn skeleton in solution. The solution conformations of these tripeptide models containing azaPhe residue were determined in $CDCl_3$ and DMSO solvents using NMR and molecular modeling techniques. The characteristic NOE patterns, the temperature coefficients of amide protons and small solvent accessibility for the azapeptides **1**–**4** reveal to adopt the β-turn structure. The structures of azapeptides containing azaPhe residue from a restrained molecular dynamics simulation indicated that average dihedral angles [(ϕ_1, ψ_1), (ϕ_2, ψ_2)] of Xaa-azaPhe fragment in azapeptide, Boc-Xaa-azaPhe-Ala-OMe were [(−68°, 135°), (116°, −1°)], and this implies that the intercalation of an azaPhe residue in tripeptide induces the βII-turn conformation, and the volume change of a preceding amino acid of azaPhe residue in tripeptides would not perturb seriously the backbone dihedral angle of β-turn conformation. We believe such information could be critical in designing useful molecules containing azaPhe residue for drug discovery and peptide engineering.

Keywords: Azapeptide; β-Turn; NMR; Molecular dynamics

1. Introduction

The modification of peptides is a general strategy for drug design to increase the resistance to physiological degradation and decrease the conformational flexibility [1]. Numerous possibilities of structure modifications considering both the peptide backbone and the amino acid side chains have been considered and proved to be promising for future drug development [2–7]. Among these modifications, the azaamino acids are promising peptidomimetic compounds, which are formed by the replacement of an α-carbon of amino acids with a nitrogen atom. Azaamino acids leading to removal of the flexibility of the parent linear peptide would provide a unique conformational property to protein structure since the loss of asymmetry associated with the α-carbon and free rotation of C–C_α bond in amino acid [4,8,9]. The conformational characterizations of azaamino acids in peptide, however, were limited to the several models for azapeptides associated with azaPro, azaGly, azaAla or azaLeu residue. [5,10–22] Although the azapeptides associated with azaPhe scaffold have already been

Abbreviations: Ac, acetyl; NMR, nuclear magnetic resonance; TOCSY, total correlation spectroscopy; NOESY, nuclear overhauser enhancement spectroscopy; MD, molecular dynamics.

* Corresponding author. Tel.: +82 2 958 5957; fax: +82 2 958 5969.
E-mail address: leekb@kist.re.kr (K.-B. Lee).

0301-4622/$ - see front matter © 2006 Published by Elsevier B.V.
doi:10.1016/j.bpc.2006.05.028

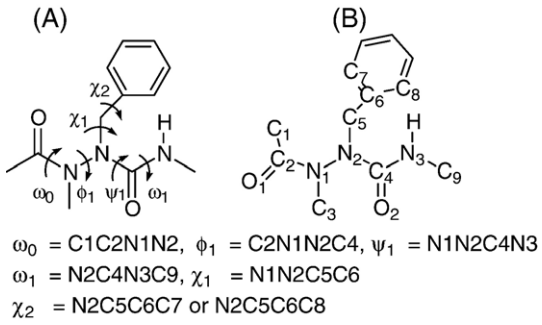

Fig. 1. The chemical structure of Ac-azaPhe-NHMe with (A) a *trans* amide orientation ($\omega_0 \sim 180°$) and (B) a *cis* amide orientation ($\omega_0 \sim 0°$).

utilized as thrombin inhibitor [9,23,24] and serine protease inhibitor [25,26], its structural aspect has not been investigated precisely.

The theoretical studies of azapeptide models, For-azaXaa-NH_2(Xaa=Gly, Ala, Leu) showed that the preferred conformations are limited to the range of stereochemically allowed backbone dihedral angle ($\phi = \pm 90° \pm 30°$, $\psi = 0° \pm 30°$ or $\pm 180° \pm 30°$) corresponding to the β-turn motif for the $i+2$ residue [4,5]. These theoretically preferred β-turn motifs of azaamino acid-containing peptides were confirmed recently using IR, and NMR and molecular modeling techniques [4,5].

However, the activities of biologically important peptides are strongly influenced by a definite structure of specific azaamino acid residue in the peptide chain, and the conformational change by the modification of azaamino residue in peptides has to be defined precisely.

Ab initio MO theory was employed to calculate the backbone dihedral angle of the most stable conformer for Ac-azaPhe-NHMe (Fig. 1) to investigate the role of azaPhe residue and the influence for the preceding residues of azaPhe in the azapeptide structure. The solution conformations of azapeptides, Boc-Xaa-azaPhe-Ala-OMe [Xaa=Gly(**1**), Ala(**2**), Phe(**3**), Asn(**4**)] (Fig. 2) using NMR and restrained molecular dynamics have been characterized to verify whether the backbone torsion angles of azaPhe reside are still the same as compared with theoretical conformations and how the preceding amino acids of azaPhe residue would perturb the β-turn backbone skeleton.

2. Experimental

2.1. Calculation method

To get insight into the conformational preferences of azaphenylalanine in peptide, we used model compound, Ac-azaPhe-NHMe. The starting conformers for azaPhe amino acid with the acetyl group oriented in a *trans*($\omega_o \sim 180°$) and *cis* ($\omega_o \sim 0°$) configuration were generated by the combination of preferred (ϕ, ψ) dihedral angles of azaAla (or azaGly) residue and probable χ_1 and χ_2 angles of (+60°, +120°, 180°, −60°, −120°). The starting conformers were fully optimized at the HF/3-21G level of theory . The HF/3-21G-resulting conformers of Ac-azaPhe-NHMe were reoptimized at the HF/6-31G* level [27]. All of the stationary points were found to be local minima, as indicated by the absence of imaginary frequencies at the HF/6-31G* level. The vibrational frequencies calculated at this level were used to compute the enthalpy and the Gibbs free energy difference at 298 K. Relative Gibbs free energies were calculated with the thermal energy and entropy corrections including zero-point energy. The single point energy calculation was also performed by B3LYP method using the HF/6-31G*-optimized geometries. To investigate the solvent effect in water ($\varepsilon = 78.39$) and in chloroform ($\varepsilon = 4.71$) on conformational stability of azaPhe, the isodensity polarizable continuum model (IPCM) method was used because its efficiency has been recognized [28]. The 0.0004 electron per cubic Bohr (e/B) electron density surface was used to define the boundary of the solute. All quantum chemical calculations were performed employing the Gaussian 94 molecular orbital package program

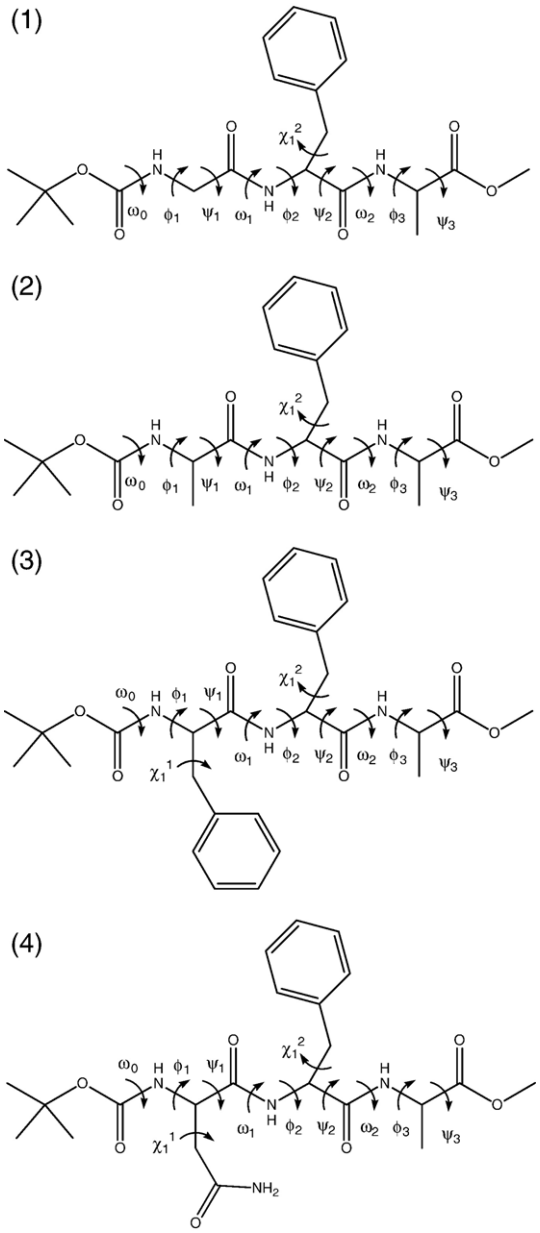

Fig. 2. Primary structure of Boc-Xaa-azaPhe-Ala-OMe [Xaa=Gly(**1**), Ala(**2**), Phe(**3**), Asn(**4**)].

[29] operated on a Pentium IV personal computer and Cray T3E supercomputer.

2.2. Peptide synthesis

HBTU, Boc-Gly, Boc-Ala, Boc-Phe, Boc-Asn, Boc-NH-NH_2 and Ala-OMe were obtained from Novabiochem (San Diego, CA, USA); 4-nitrophenyl chloroformate, TFA and Isobutanal were obtained from Aldrich (St. Louis, MO, USA); peptide grade DCM and DIEA were obtained from ABI (Foster, CA, USA). Boc-azaPhe-Ala-OMe was prepared as described previously [4]. After removal of Boc group from the Boc-azaPhe-Ala-OMe (41.7 mg, 0.09 mmol) by 30% TFA in DCM, the resulting peptide was coupled to Boc-Xaa (15.0 mg, 0.079 mmol) using HBTU (33.0 mg, 0.08 mmol) and DIEA (0.03 mL, 0.19 mmol) in DMF. After confirming the disappearance of the starting material by TLC, the solvent was evaporated *in vacuo*. The residue was dissolved in EtOAc and the solution was washed with saturated solution of $NaHCO_3$ and 10 % $KHSO_4$. The solution was dried over anhydrous $MgSO_4$ and evaporated to dryness *in vacuo*. The desired products were separated by silica gel chromatography.

2.3. NMR spectroscopy

All NMR experiments were performed using a 5 mm indirect probe on Varian Unity *plus* 600 spectrometer operating at a ^1H frequency of 599.9 MHz. The sample concentration was made to 2–5 mM in $CDCl_3$ or DMSO-d_6 solvent. The ^1H NMR experiment was collected with 32 K data points, and zero-filled to 64 K data points to measure the coupling constants. For variable temperature experiments, the sample allowed to equilibrate in the probe for 20–30 min before data collection over the temperature range form 283 K to 313 K in $CDCl_3$ solvent. Two-dimensional TOCSY and NOESY were acquired. NOESY spectra were recorded with mixing times of 100, 150, 200, 300, 500, 700 ms and displayed in the phase-sensitive mode. The chemical shifts were referenced to tetramethylsilane (TMS, 0.0 ppm). All NMR data sets were processed using the VNMR 5.1 software on Indigo II workstation.

2.4. Molecular modeling

To get the distance information, NOE volumes were measured and averaged on both sides of the diagonal, and these NOE volumes were translated into interproton distances at the NOESY spectrum with mixing time of 150 ms. In this procedure, the NOE volume of cross-peaks involving a methyl group was divided by 3 (or 9 for NOEs between two methyl groups). The range of the upper and lower constraints was set to ±5% using Phe $C^{\beta}{}^1H/C^{\beta}{}^2H$ cross peaks (1.80 Å) as a reference. This variation allows some errors in the measurement of the volume of cross peaks and their conversion into distance restraints. Structural calculations were performed using a restricted molecular dynamics simulation based on NOEs and hydrogen bond restraints (NH–O=1.8–2.7 Å and N–O=2.5–3.7 Å) [4]. Based on cross peak intensities in the NOESY spectra with mixing times of 100–700 ms, the distance constraints were classified as strong (2.0–2.5 Å), medium (2.5–3.0 Å) and weak (3.0–4.0 Å) NOEs. Pseudoatom corrections were used for methylene protons, methyl groups and the ring protons of phenylalanine residue.

NOE restrained simulated annealing protocol in SYBYL 6.3 (Tripos, Inc., 1699 South Hanley Rd., St. Louis, MO 63144,

Table 1
Dihedral angles, calculated dipole moment, and relative energies (ΔE at 0 K, in kcal/mol), enthalpy (ΔH at 298 K, in kcal/mol) and Gibbs energies (ΔG at 298 K, in kcal/mol) of Ac-azaPhe-NHMe at the HF/6-31G* level in gas and solution (water and $CHCl_3$) phases

Conformation	ω_0	ϕ	ψ	ω_1	χ_1	χ_2	ΔE[a]	ΔE[b]	ΔH[a]	ΔG[a]	μ	ΔE[c] (ε=78.39)	ΔE[c] (ε=4.71)	Structure[d]
AFt1	165	−69	161	178	55	61	4.33	5.13	4.30	3.73	2.6	5.12	7.73	$\beta_P(g^+)$[e]
AFt2	160	−69	171	172	129	142	3.13	5.59	4.68	3.40	3.8	6.24	7.80	$\beta_P(a)$
AFt3	163	−87	176	−174	65	72	4.64	3.68	3.06	3.03	3.1	8.27	9.55	$\varepsilon''(g^+)$
AFt4	161	−87	−176	−174	−126	38	2.57	2.34	2.68	2.87	3.2	5.54	7.61	$\varepsilon'(a)$
AFt5	−166	−115	10	171	66	68	1.13	1.43	1.09	0.09	5.4	2.92	5.19	$\delta_R(g^+)$
AFt6	−175	−96	28	172	−130	45	5.27	4.70	5.12	3.96	4.8	5.20	8.40	$\delta_R(a)$
AFt7	−168	−94	28	172	−58	133	3.45	3.15	3.26	2.61	4.6	0.00[j]	5.99	$\delta_R(g^-)$
AFc1	−21	−72	−173	175	102	−44	5.49	5.52	5.42	5.30	9.6	4.10	6.77	$\varepsilon'(g^+)$
AFc2	−22	−81	−165	−173	−142	−144	6.13	5.63	6.08	6.24	9.3	6.21	0.00[k]	$\varepsilon'(a)$
AFc3	22	−117	15	−177	64	79	0.00[f]	0.00[g]	0.00[h]	0.00[i]	0.7	4.01	4.98	$\delta_R(g^+)$
AFc4	23	−109	8	−177	−86	106	1.92	1.49	1.84	1.38	0.5	10.38	1.42	$\delta_R(g^-)$

[a] HF/6-31G*//HF/6-31G*.
[b] B3LYP/6-31G*//HF/6-31G*.
[c] IPCM/HF/6-31G*//HF/6-31G*.
[d] Ref. [30].
[e] Ref. [35].
[f] E=−738.373696 au.
[g] E=−742.909240 au.
[h] E=−738.081372 au.
[i] E=−738.142137 au.
[j] E=−738.404310 au.
[k] E=−738.397770 au.

USA) was carried out from randomized coordinates in the first iteration. The average structure taken from the 20 structures in the previous iteration was used as the starting structure for the later iterations. The detailed method of a restrained molecular dynamics simulation was described in the previous work [4]. The best 18 structures among the obtained 50 structures consistent with experimental data were selected and analyzed.

3. Results and discussion

3.1. Minimum energy conformations

The HF/3-21G-optimized structures for Ac-azaPhe-NHMe obtained with different methods provided 24 minima at $\omega_o \sim 180°$ and 8 minima at $\omega_o \sim 0°$, respectively. If one ignores mirror image, the minimum energy conformations become 12 minima at $\omega_o \sim 180°$ and 4 minima at $\omega_o \sim 0°$, respectively (not shown). These conformations were used as starting points for full optimization at the HF/6-31G* level and led to 7 at $\omega_o \sim 180°$ and 4 minima at $\omega_o \sim 0°$ as displayed in Table 1 and Fig. 4. Table 1 contains the backbone ϕ_1 and ψ_1 angles and side chain χ_1 and χ_2 angles of the HF/6-31G* minima for Ac-azaPhe-NHMe. The notations for the structures in Table 1 are generally accepted for characteristic regions of peptide (ϕ, ψ) space in protein crystallography (Fig. 3) [30]. According to the backbone dihedral angle, the HF/6-31G*-optimized structures can be classified into 4 groups: β_P (polyproline II; $\phi \sim -78°$, $\psi \sim 149°$), ε' and ε'' (extend; $\phi > 0$, $\psi = \pm 180°$), and δ_R (bridge; $\phi \sim -90°$, $\psi \sim 0°$). The side chain conformations were defined as gauche plus (g^+), anti(a), or gauche minus (g^-) depending on the dihedral χ_1 angles.

As shown in Table 1, the backbone conformations for the minima of Ac-azaPhe-NHMe [$\phi = \pm 91° \pm 24°$, $\psi = \pm 18° \pm 10°$ (or $\pm 69° \pm 8°$)] are similar to those of Ac-azaAla-NHMe ($\phi \sim \pm 91°$, $\psi \sim \pm 165°$ or ± 1) reported earlier [8,19,31]. These favorable dihedral ϕ and ψ angles can be explained by the repulsion between nitrogen lone pairs and amide conjugation effect [8,32,33]. However, the subtle difference in backbone dihedral angle of Ac-azaPhe-NHMe as compared to that of Ac-azaAla-NHMe appears to be related with an orientation of the aromatic side chain. Since the backbone of Ac-azaPhe-NHMe is restricted, this implies that its side chain χ_1 and χ_2 angles can also be restricted.

For **AFt** with a *trans* amide bond of acethyl group, **AFt1** and **AFt2** adopt the β_P conformation, which prefer the 55° (g^+) or 129° (a), respectively. The χ_1 angle of −60° (g^-) in the β_P conformation is not allowed because of a steric bump between phenyl group and the N-terminal carbonyl group (conformer I in

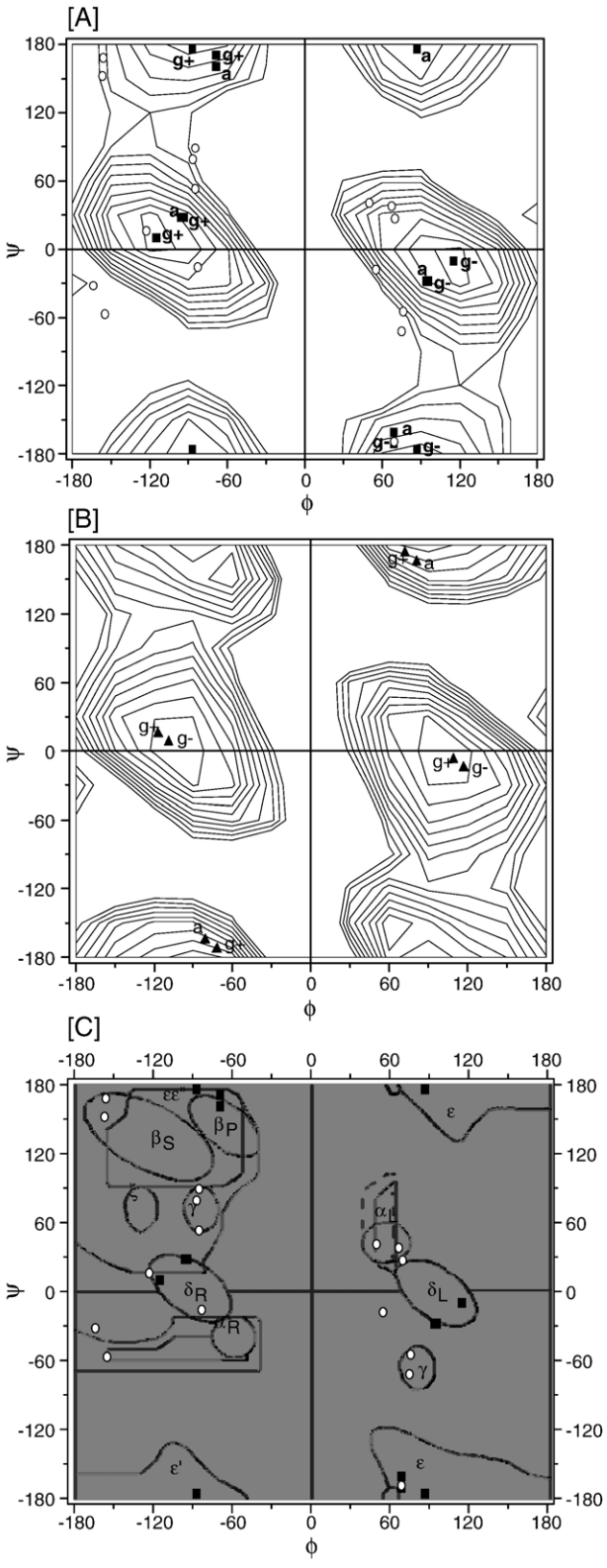

Fig. 3. The distribution of the backbone dihedral angles (ϕ_1, ψ_1) for the minimum energy conformations of Ac-Phe-NHMe (○) [35] and Ac-azaPhe-NHMe (■). **HF/6-31G*** potential energy surfaces of Ac-azaAla-NHMe [31] for a *trans* amide orientation ($\omega_0 \sim 180°$) [A] and for a *cis* amide orientation ($\omega_0 \sim 0°$) [B]. Geometry optimization of all variables except ϕ_1 and ψ_1 were performed on a grid with 30° spacing. Solid contours are drawn every 1 kcal/mol from the global minimum to 10 kcal/mol. [C] Allowed and partly allowed regions of native conformations and nomenclatures were taken in Karplus [30] (α_R, right-handed α-helix; α_L, mirror image of α-helix; β_S, region largely involved in β-sheet formation; β_P, regions associated with extended polyproline-like helix or β-sheet; γ and γ', γ and inverse-γ turns; δ_R, the bridge region; δ_L, mirror image of δ_R region; ε, extensive region with $\phi > 0$, $\varphi = \pm 180°$; ε' and ε'', mirror images of the two parts of the ε region; ζ, a region associated with residues preceding Pro).

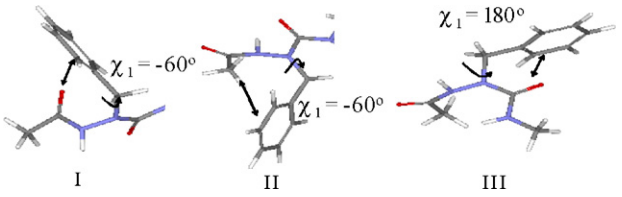

Scheme 1.

Scheme 1). This unfavorable conformer I was converged into the conformer **AFt4** as it was optimized at the HF/6-31G* level. This shows that the difference of backbone angles between **AFt1** and **AFt4** is cause by the configurational difference of the aromatic chain.

The preferred χ_1 angle for the conformers **AFt3** and **AFt4**, which adopt the ε conformation, can be explained by the similar reasons to the conformers **AFt1** and **AFt2**. The orientation of phenyl group toward carbonyl group in the conformer **AFt4**

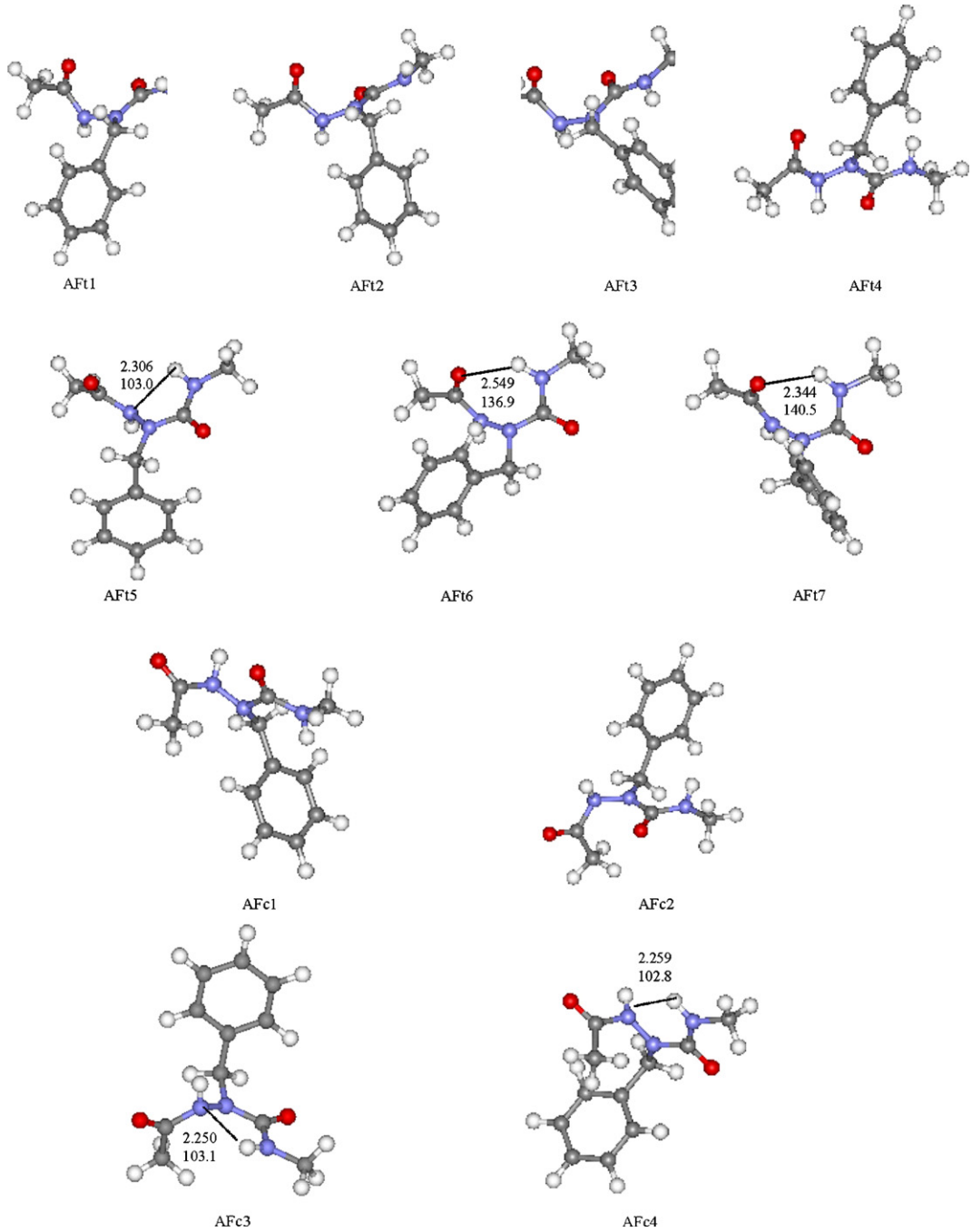

Fig. 4. HF/6-31G* minima of Ac-azaPhe-NHMe. The geometries with the intramolecular hydrogen bonding parameters are included. Each atoms in molecules are colored with red (oxygen), blue (nitrogen), black (nitrogen) and white (hydrogen). (For interpretation of the references to colour in this figure legend, the reader is referred to the web version of this article.)

seems to be due to induced polarization of phenyl ring CH by the carbonyl group.

The conformers **AFt5**, **AFt6,** and **AFt7** adopt the δ_R conformation (Table 1). The conformer **AFt5** has an intramolecular 5-membered hydrogen-bond ring: the H–N distance of 2.306 Å and the N–H–N angle of 100.3° (Fig. 4). For the conformers **AFt6** and **AFt7**, a 7-membered hydrogen-bond ring was found. The O–H hydrogen bond distance for **AFt7** is shorter than that for **AFt6**. The plausible conformer that has *a* or *g*-orientation of the side chain for **AFt5** was converged into **AFt6** or **AF7** conformer, respectively, when it was re-optimized at the HF/6-31G* level. This is true for vice verse. This implies that the 7-membered hydrogen-bond ring plays a role in determining the backbone angle of **AFt6** and **AFt7**.

For **AFc** ($\omega_o \sim 0°$) with a *cis* amide bond of acethyl group, four minima were generated The conformers, **AFc1** and **AFc2** adopt an extended (ε) conformation, and **AFc3** and A**Fc4** adopt δ_R structure. In the case of **AFc1** and **AFc2**, the χ_1 angle of $-60°$ (g^-) configuration is not found because of a steric bump between benzyl group and N-terminal methyl group (conformer **II** in Scheme 1). For **AFc3** or **AFc4**, the χ_1 angle of 180° (*a*) configuration is destabilized because of a steric bump between benzyl group and C-terminal carbonyl group (conformer **III** in Scheme 1).

Although a *trans* peptide bond is more favorable than a *cis* peptide bond in natural peptides, it is not always the case in azapeptides as reported earlier [20,31]. Table 1 contains the relative enthalpies and free energies of gas-phase conformers calculated from the HF/6-31G* geometries for Ac-azaPhe-NHMe. The lowest energy conformation for Ac-azaPhe-NHMe is determined to be **AFc3** at the HF/3-21G and HF/6-31G* levels or by a single-point energy calculation at the B3LYP/6-31G*//HF/6-31G* level. The relative enthalpy and Gibbs energy also indicate that **AFc3** is the global minimum (Fig. 4 and Table 1). The second lowest conformer is **AFt5**. The relative energies between minima calculated by the solvation IPCM model showed that the conformer **AFt7** or **AFc2** is the most stable in water (ε=78.4) or $CHCl_3$ (ε=4.17) solution, respectively. The experimental 3D structure of Boc-azaPhe-azaGly-ACHPA-azaIle-3-pyridylmethylamide containing azaPhe residue by X-ray crystallography indicated that the respective backbone ϕ, ψ and χ_1 angles of azaPhe residue in this azapeptide are $-109°$, 11° and 70°, which is well-consistent with **AFt5** conformation. The results suggested that the conformational preference of azaPhe-residue would be changed by solvent or neighbor residue.

3.2. The preferred conformations of azaPhe residue with respect to Phe residue

To investigate the effect of structural changes by the replacement of an alpha carbon with a nitrogen atom, the distribution of the backbone dihedral angles for the minimum energy conformations of Phe- and azaPhe-containing model peptides was displayed (Fig. 3) [34–36]. The open circles represent the minima for phenylalanine-containing peptide model and the solid square is the minima for azaPhe-containing peptide model [35,36]. Jákli et al. noticed that the predicted minima for Phe-containing peptide model showed a good agreement with the available X-ray data [36]. They found that polyproline II (β_P) structure and right-handed α-helix structure (α_R) are not a local minimum for Phe. In the case of azaPhe-containing peptide model, note that the β_P structure is one of the minima. Whereas the β-strand (β_S) structure is the global minimum for Phe, this is destabilized for azaPhe. The preferential χ_1 and χ_2 angles for azaPhe model are significantly different with those for Phe model. In the case of Phe model, most of minimum energy conformations allowed the g^+, *a*, g^- configuration of aromatic side chain. However, the configuration of the aromatic side chain in azaPhe is restricted. This is caused by the bias backbone conformation. Since the ϕ bond adopts 90°, the N1–C^β bond is perpendicular to the N-terminal amide group. Thus, the orientation of side chain leads to a steric hindrance with the N-terminal carbonyl group or the C-terminal amide NH group as discussed previously (see Scheme 1).

3.3. Solution conformation of Boc-Xaa-azaPhe-Ala-OMe

In order to substantiate experimentally whether this theoretical β-turn motif for azaPhe residue is still conserved in solution, we have designed and synthesized azapeptides containing azaPhe residue, Boc-Xaa-azaPhe-Ala-OMe [Xaa=Gly(**1**), Ala(**2**), Phe(**3**), Asn(**4**)] as shown in Fig. 2, and the solution conformations of these azapeptides were characterized using NMR spectroscopy and molecular modeling method.

All proton resonances were unambiguously assigned with the peak intensities, TOCSY and sequential NOEs observed in NOESY spectrum. The observed proton chemical shifts of azapeptides, **1–4** are displayed in Table 2. To get a detailed information about conformations of azapeptides **1–4**, 2D-NOESY data with the different mixing times were collected and analyzed. Fig. 5 shows the NOESY spectra for azapeptide **1–4**. A number of sequential $d_{NN}(i, i+1)$ NOEs are observed in the whole segment, which indicate azapeptides **1–4** associated with azaPhe residue adopt a folded conformation. A strong NOE between ^{1}Xaa $C^\alpha H$ and ^{2}azaPhe, and a medium NOE between

Table 2
Chemical shifts for protons of **1–4** in $CDCl_3$ at 25 °C

Model	Residues	NH	αH	βH	Others
1	^{1}Gly	5.03	3.70		Boc 1.43
	^{2}azaPhe	7.71	–	4.93, 4.58	Ring Hs 7.32–7.24
	Ala	6.05	4.49	1.43	–OMe 3.73
2	^{1}Ala	4.75	3.82	1.22	Boc 1.40
	^{2}azaPhe	7.63	–	4.90, 4.46	Ring Hs 7.33–7.28
	^{3}Ala	6.15	4.44	1.38	–OMe 3.69
3	^{1}Phe	4.80	3.98	3.03,2.91	Boc 1.86
					Ring Hs 7.17, 7.09
	^{2}azaPhe	7.40	–	4.92, 4.25	Ring Hs 7.38, 7.30
	^{3}Ala	6.17	4.49	1.40	–OMe 4.22
4	^{1}Asn	5.21	4.09	2.93	Boc, 1.63 γNH_2 4.91
	^{2}azaPhe	7.95	–	4.94, 4.47	Ring Hs 7.32–7.25
	^{3}Ala	6.00	4.47	1.40	–OMe 3.69

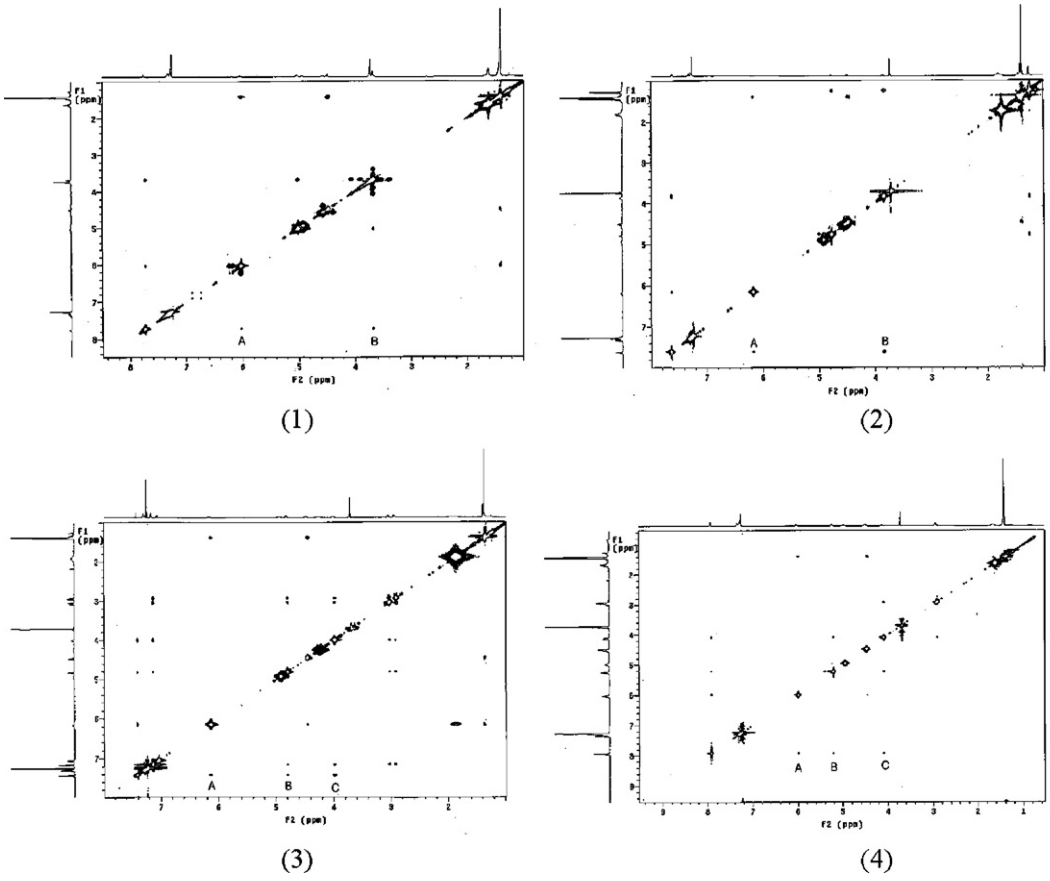

Fig. 5. NOESY spectra (mixing time = 700 ms) of **1** (A: ^{2}azaPhe NH ↔ ^{3}Ala NH, B: ^{2}azaPhe NH ↔ ^{1}Gly C$^{\alpha}$H), **2** (A: ^{2}azaPhe NH ↔ ^{3}Ala NH, B: ^{2}azaPhe NH ↔ ^{1}Ala C$^{\alpha}$H), **3** (A: ^{2}azaPhe NH ↔ ^{3}Ala NH, B: ^{2}azaPhe NH ↔ ^{1}Phe NH, C: ^{2}azaPhe NH ↔ ^{1}Phe C$^{\alpha}$H), **4** (A: ^{2}azaPhe NH ↔ ^{3}Ala NH, B: ^{2}azaPhe NH ↔ ^{1}Asn NH, C: ^{2}azaPhe NH ↔ ^{1}Asn C$^{\alpha}$H) azapeptides in $CDCl_3$ solvent.

^{2}azaPhe NH and ^{4}Ala NH (Table 3 and Fig. 6) indicate that azapeptides, **1–4** adopts the *β*II-turn structure. However, the presence of a weak NOE between ^{1}Asn NH and ^{2}azaPhe NH suggests that azapeptide **4** partially adopts *β*I-turn structure although we are unable to determine relative ratio between *β*I- and *β*II-turn structures (Scheme 2). In order to evaluate the exact ratio between *β*I- and *β*II-turn structures in azapeptides **1–4**, we have taken CD spectra in $CDCl_3$ solvent since those peptides were not dissolved in water. However, the CD spectra were not interpreted by unusual form of CD spectra due to organic

Table 3
NOE volume integrals of the azapeptide **1–4** in $CDCl_3$ solution

NOE connectivities	NOE volume ($\times 10^4$)[a]	NOE connectivities	NOE volume ($\times 10^4$)[a]	NOE connectivities	NOE volume ($\times 10^4$)[a]	NOE connectivities	NOE volume ($\times 10^4$)[a]
Boc-Gly-azaPhe-Ala-NHMe (1)		**Boc-Ala-azaPhe-Ala-NHMe (2)**		**Boc-Phe-azaPhe-Ala-NHMe (3)**		**Boc-Asn-azaPhe-Ala-NHMe (4)**	
^{1}Gly NH – ^{1}Gly C$^{\alpha}$H	−7.93	^{1}Ala NH – ^{1}Ala C$^{\beta}$H$_3$	−10.93	^{1}Phe NH – ^{1}Phe C$^{\beta 1}$H	−2.57	^{1}Asn NH – ^{1}Asn C$^{\alpha}$H	−4.56
		^{1}Ala C$^{\alpha}$H – ^{1}Ala C$^{\beta}$H$_3$	−6.96	^{1}Phe NH – ^{1}Phe C$^{\beta 2}$H	−3.53	^{1}Asn NH – ^{1}Asn C$^{\beta}$H	−2.37
				^{1}Phe NH – ^{1}Phe ^{2,6}H	−1.96	^{1}Asn C$^{\alpha}$H – ^{1}Asn C$^{\beta}$H	−5.53
				^{1}Phe C$^{\alpha}$H –^{1}Phe C$^{\beta 1}$H	−2.36		
				^{1}Phe C$^{\alpha}$H – ^{1}Phe C$^{\beta 2}$H	−2.16		
				^{1}Phe C$^{\alpha}$H – ^{1}Phe ^{2,6}H	−3.70		
				^{1}Phe C$^{\beta 1}$H – ^{1}Phe C$^{\beta 2}$H	−13.49		
				^{1}Phe C$^{\beta 1}$H – ^{1}Phe ^{2,6}H	−4.25		
				^{1}Phe NH – ^{2}azaPhe NH	−2.54	^{1}Asn NH – ^{2}azaPhe NH	−3.69
^{1}Gly C$^{\alpha}$H – ^{2}azaPhe NH	−6.17	^{1}Ala C$^{\alpha}$H – ^{2}azaPhe NH	−6.68	^{1}Phe C$^{\alpha}$H –^{2}azaPhe NH	−11.04	^{1}Asn C$^{\alpha}$H – ^{2}azaPhe NH	−6.68
^{2}azaPhe NH – ^{3}Ala NH	−4.09	^{2}azaPhe NH – ^{3}Ala NH	−3.11	^{2}azaPhe NH – ^{3}Ala NH	−2.97	^{2}azaPhe NH – ^{3}Ala NH	−6.17
^{3}Ala C$^{\alpha}$H – ^{3}Ala C$^{\beta}$H$_3$	−16.89	^{3}Ala NH – ^{3}Ala C$^{\beta}$H$_3$	−2.84	^{3}Ala NH – ^{3}Ala C$^{\alpha}$H$_3$	−2.13	^{3}Ala NH – ^{3}Ala C$^{\alpha}$H$_3$	−3.30
				^{3}Ala NH – ^{3}Ala C$^{\beta}$H$_3$	−3.78	^{3}Ala NH – ^{3}Ala C$^{\beta}$H$_3$	−7.12
				^{3}Ala C$^{\alpha}$H –^{3}Ala C$^{\beta}$H$_3$	−7.92		

[a] The distance restraints used in the restricted simulated annealing calculations of azapeptide.

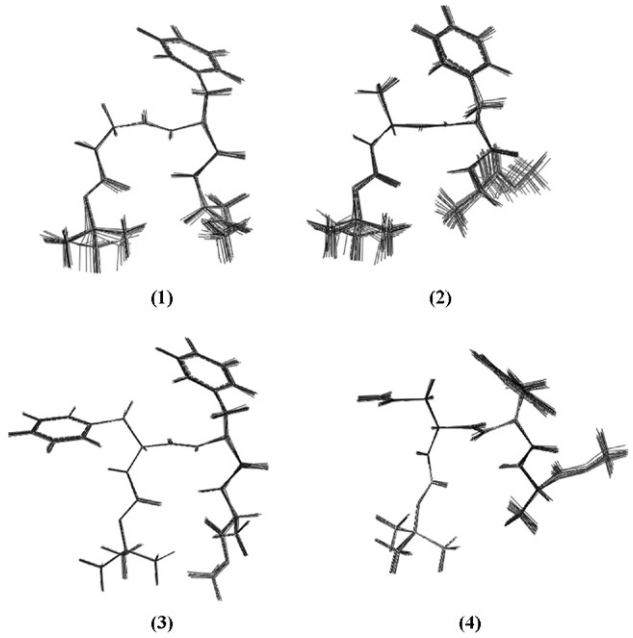

Fig. 6. The 18 superimposed structures of Boc-Xaa-azaPhe-Ala-OMe [(Xaa=Gly(**1**), Ala(**2**), Phe(**3**), Asp(**4**)).

solvent unlike usual CD spectral forms of peptides dissolved in water.

In order to confirm whether the intramolecular hydrogen bonding in peptide exists, the chemical shift and temperature dependence for the amide protons were measured in $CDCl_3$ and DMSO-d_6 solvents. Since it has been known that the intramolecular H-bonding and free amide protons of normal peptides in nonpolar solvents resonate at 7–9 and 4–6 ppm, respectively, the amide proton of azapeptides seems not to be involved in intramolecular hydrogen bonding (Table 4). The urea-type ^{3}Ala NH of azapeptides, **1–4** resonating at ~6.1 ppm seems to be involved in intramolecular hydrogen bonding since the hydrogen-bonded urea type NH resonates at 5.62 ppm in $CDCl_3$. As shown in Table 4, the ^{3}Ala NH of azapeptides **1–4** shows the relatively larger temperature dependence, as

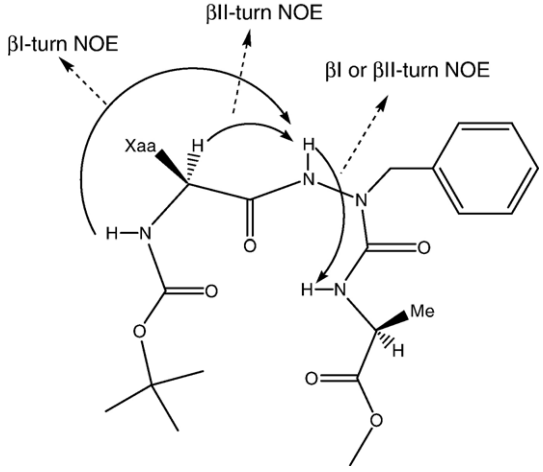

Scheme 2.

Table 4
Temperature coefficients and solvent accessibility for amide protons of **1–4**

Peptides	Residues	$\Delta\delta/\Delta T$ ($CDCl_3$)[a]	Solvent accessibility[b]
1	^{1}Gly	−2.4	2.08
	^{2}azaPhe	−5.9	2.35
	^{3}Ala	−4.9	0.72
2	^{1}Ala	−1.7	2.39
	^{2}azaPhe	−4.8	2.56
	^{3}Ala	−4.7	0.31
3	^{1}Phe	−1.6	[c]
	^{2}azaPhe	−3.6	2.85
	^{3}Ala	−6.0	0.26
4	^{1}Asn	−4.6	2.37
	^{2}azaPhe	−6.8	2.53
	^{3}Ala	−5.4	0.61
Ref	^{1}Phe	−5.6	2.31
	^{2}azaLeu	−6.1	2.50
	^{3}Ala	−1.9	0.26

[a] In unit of ppb/K.
[b] $\delta_{NH \text{ in DMSO-d6}} - \delta_{NH \text{ in } CDCl_3 \text{ solution}}$.
[c] Not determined.

compared with ^{3}Ala NH of Boc-Phe-azaLeu-Ala-OMe, but small solvent accessibility. Given that the intramolecular NOE pattern, NH chemical shift, and small solvent accessibility of ^{3}Ala NH indicates clearly that azapeptides **1–4** adopt a folded structure, large temperature dependence of ^{3}Ala NH may result from unfolding as the temperature is increased in $CDCl_3$, suggested by Stevens et al. [37].

The molecular modeling calculations were performed using NOE constraints derived from NMR spectrum to characterize the microstructure of azapeptides, **1–4** in solution state. The initial calculation showed that the possible hydrogen bonding

Table 5
The selected dihedral angles of the azapeptide **1–4** by restrained molecular dynamics simulations

1	^{1}Gly	Dihedral angle	^{2}azaPhe	Dihedral angle
	ϕ_1	−65 (±6)	ϕ_2	115 (±2)
	ψ_1	119 (±2)	ψ_2	−10 (±3)
	ω_1	169 (±3)	ω_2	155 (±2)
	χ_1^1	–	χ_1^2	−66 (±2)
2	^{1}Ala	Dihedral angle	^{2}azaPhe	Dihedral angle
	ϕ_1	−67 (±6)	ϕ_2	115 (±2)
	ψ_1	142 (±5)	ψ_2	−10 (±3)
	ω_1	171 (±3)	ω_2	152 (±3)
	χ_1^1	–	χ_1^2	−66 (±2)
3	^{1}Phe	Dihedral angle	^{2}azaPhe	Dihedral angle
	ϕ_1	−69 (±1)	ϕ_2	115 (±3)
	ψ_1	117 (±1)	ψ_2	−10 (±2)
	ω_1	166 (±3)	ω_2	168 (±2)
	χ_1^1	−40 (±1)	χ_1^2	−66 (±2)
4	^{1}Asn	Dihedral angle	^{2}azaPhe	Dihedral angle
	ϕ_1	−69 (±2)	ϕ_2	116 (±3)
	ψ_1	113 (±1)	ψ_2	9 (±4)
	ω_1	169 (±2)	ω_2	147 (±3)
	χ_1^1	−62 (±1)	χ_1^2	−66 (±3)

[a]The standard deviationof dihedral angle in 18 superimposed structures.

acceptor for the amide proton of ^{3}Ala residue is the carbonyl oxygen of ^{1}Xaa residues. Thus, a hydrogen bond constraint was additionally introduced for the high quality structure refinement, and their NMR structures in Fig. 5 display the best 18 superimposed structures for the azapeptides, **1–4** generated by restrained molecular dynamics simulations with NOEs and H-bond constraints. The backbone mean RMSDs of the 18 superimposed structures is 0.81±0.10 Å, and the azapeptides **1–4** adopt *β*II-turn conformation. As shown in Table 5, the average dihedral angle (ϕ_1, ψ_1, ω_1, χ_1^1) of Xaa residue in azapeptides, **1–4** are found to be (−68°±6°, 123°±5°, 168°±3°, 51°±1°), and the average dihedral angle, (ϕ_2,ψ_2, ω_2, χ_1^2) of azaPhe residue is (116°±2°, −6°±1°, 156°±10°, −66°±11°). This fact suggests that the change of preceding amino acids of azaPhe residue would not influence much the backbone structure of azapeptide since the phenyl ring of ^{1}Phe or the side chain of ^{1}Asn residue and the side chain of ^{2}azaPhe residue are located far each other. The aromatic side chain χ_1 angle of azaPhe residue preferentially adopts between ±60° and ±130° due to a steric bump between the N(or C)-terminal carbonyl group or the N(or C)-terminal amide methyl group and the aromatic side chain. The optimized structures for azaPhe are different from those of normal peptide containing Phe residue (Fig. 3). The conformations of Boc and NHMe groups in the restrained molecular dynamics structures are not well-defined as shown in Fig. 6, since the terminals of peptides and proteins are usually very flexible.

In conclusion, we performed the *ab initio* calculation on the conformation of the Ac-azaPhe-NHMe, and its theoretical conformation was compared with that of Ac-Phe-NHMe to investigate the influence of Phe group in the structure of azapeptide. The calculated structure for Ac-azaPhe-NHMe demonstrated that the incorporation of azaPhe residue in designed azapeptide would not perturb the backbone dihedral angles of azapeptide occurring at the stable *β*-turn structure. As expected by theoretical calculation, the solution structure of the designed azapeptides including azaPhe residue clearly indicated that the intercalation of azaPhe residue in synthetic tripeptide provides the stable *β*II-turn structure in $CDCl_3$. Therefore, these findings suggest that azaamino acids could be utilized in designing new peptidomimetics adopting *β*-turn scaffold.

Acknowledgments

This work was supported by grants from Korean Ministry of Health and Welfare (2M12330) to K.-B. Lee.

References

[1] M. Goodman, S. Ro, Burger's medicinal chemistry and drug discovery, in: M.E. Wolff (Ed.), Principles and Practice, 5th ed., John Wiley and Sons, Inc., New York, 1995, pp. 803–861.
[2] M. Chorev, M. Goodman, A dozen years of retro-inverso peptidomimetics, Accounts of Chemical Research 26 (1993) 266–273.
[3] V.J. Hruby, G.G. Li, C. HaskellLuevano, M. Shenderovich, Design of peptides, proteins, and peptidomimetics in chi space, Biopolymers 43 (1997) 219–266.
[4] H.J. Lee, I.A. Ahn, S. Ro, K.H. Choi, Y.S. Choi, K.B. Lee, Role of azaamino acid residue in *β*-turn formation and stability in designed peptide, J. Pept. Res. 56 (2000) 35–46.
[5] H.J. Lee, K.H. Choi, I.A. Ahn, S. Ro, H.G. Jang, Y.S. Choi, K.B. Lee, The *β*-turn preferential solution conformation of a tetrapeptide containing an azaamino acid residue, J. Mol. Struct. 569 (2001) 43–54.
[6] T.T. Tran, J. Zeng, H. Treutlein, A.W. Burgess, Effects of thioamide substitutions on the conformation and stability of alpha- and 3(10)-helices, J. Am. Chem. Soc. 124 (2002) 5222–5230.
[7] H.J. Lee, J.H. Kim, H.J. Jung, K.Y. Kim, E.J. Kim, Y.S. Choi, C.J. Yoon, Computational study of conformational preferences of thioamide-containing azaglycine peptides, J. Comput. Chem. 25 (2004) 169–178.
[8] M. Thormann, H.J. Hofmann, Conformational properties of azapeptides, J. Mol. Struct., Theochem 469 (1999) 63–76.
[9] A. Zega, U. Urleb, Azapeptides, Acta Chim. Slov. 49 (2002) 649–662.
[10] A. Lecoq, G. Boussard, M. Marraud, A. Aubry, The couple pro/azapro – a means of *β*-turn formation control synthesis and conformation of 2 azapro-containing dipeptides, Tetrahedron Lett. 33 (1992) 5209–5212.
[11] A. Lecoq, G. Boussard, M. Marraud, A. Aubry, Crystal-state conformation of 3 azapeptides containing the azaproline residue, a *β*-turn regulator, Biopolymers 33 (1993) 1051–1059.
[12] G. Boussard, A. Lecoq, A. Aubry, M. Marraud, Azaproline – a *β*-turn inducing residue opposed to proline, J. Cell. Biochem. (1993) 229.
[13] F. Pinnen, G. Luisi, A. Calcagni, G. Lucente, E. Gavuzzo, S. Cerrini, Approaches to pseudopeptidic ergopeptines: 2. Consequences of the incorporation of an α-azaproline residue into the oxacyclolic system, J. Chem. Soc., Perkin Trans. 1 (1994) 1611–1617.
[14] M. Borloo, K. Augustyns, A. Belyaev, I. deMeester, A.M. Lambeir, F. Goossens, W. Bollaert, P. Rajan, S. Scharpe, A. Haemers, Synthesis and evaluation of azaproline peptides as potential inhibitors of dipeptidyl peptidase IV and prolyl oligopeptidase, Lett. Pept. Sci. 2 (1995) 198–202.
[15] G.P. Zecchini, M.P. Paradisi, I. Torrini, G. Lucente, G. Mastropietro, M. Paci, S. Spisani, Chemotactic peptide analogues – centrally constrained chemotactic *N*-formyltripeptides: synthesis, conformation, and activity of two new analogues, Arch. Pharm. 329 (1996) 517–523.
[16] A. Bac, K. Rivoal, M.T. Cung, G. Boussard, M. Marraud, B. Soudan, D. Tetaert, P. Degand, Conformational disturbance induced by AzPro/Pro substitution in peptides, Lett. Pept. Sci. 4 (1997) 251–258.
[17] C. Didierjean, V. DelDuca, E. Benedetti, A. Aubry, M. Zouikri, M. Marraud, G. Boussard, X-Ray structures of aza-proline-containing peptides, J. Pept. Res. 50 (1997) 451–457.
[18] M. Zouikri, A. Vicherat, A. Aubry, M. Marraud, G. Boussard, Azaproline as a *β*-turn-inducer residue opposed to proline, J. Pept. Res. 52 (1998) 19–26.
[19] S. Ro, C.J. Yoon, Conformational preference of acetyl-azaalanine-*N*-methyl amide, Z. Phys. Chem. 214 (2000) 1699–1706.
[20] H.J. Lee, J.W. Song, Y.S. Choi, S. Ro, C.J. Yoon, The energetically favorable *cis* peptide bond for the azaglycine-containing peptide: for-AzGly-NH_2 model, Phys. Chem. Chem. Phys. 3 (2001) 1693–1698.
[21] W.J. Zhang, A. Berglund, J.L.F. Kao, J.P. Couty, M.C. Gershengom, G.R. Marshall, Impact of azaproline on amide *cis–trans* isomerism: conformational analyses and NMR studies of model peptides including TRH analogues, J. Am. Chem. Soc. 125 (2003) 1221–1235.
[22] Y. Che, G.R. Marshall, Impact of azaproline on peptide conformation, J. Org. Chem. 69 (2004) 9030–9042.
[23] A. Zega, G. Mlinsek, P. Sepic, S.G. Grdadolnik, T. Solmajer, T.B. Tschopp, B. Steiner, D. Kikelj, U. Urleb, Design and structure–activity relationship of thrombin inhibitors with an azaphenylalanine scaffold: potency and selectivity enhancements via P2 optimization, Bioorg. Med. Chem. 9 (2001) 2745–2756.
[24] A. Zega, G. Mlinsek, T. Solmajer, A. Trampus-Bakija, M. Stegnar, U. Urleb, Thrombin inhibitors built on an azaphenylalanine scaffold, Bioorg. Med. Chem. Lett. 14 (2004) 1563–1567.
[25] A. Obreza, M. Stegnar, A. Trampus-Bakija, A. Prezelj, U. Urleb, Synthesis and in vitro evaluation of new azaphenylalanine derivatives as serine protease inhibitors, Pharmazie 59 (2004) 739–743.
[26] A. Obreza, M. Stegnar, U. Urleb, Novel non-covalent azaphenylalanine thrombin inhibitors with an amino-methyl or amino group at the P1 position, Pharmazie 59 (2004) 659–667.

[27] M.J. Frisch, J.A. Pople, J.S. Binkley, Self-consistent molecular-orbital methods: 25. Supplementary functions for gaussian-basis sets, J. Chem. Phys. 80 (1984) 3265–3269.
[28] H.J. Lee, H.J. Jung, J.H. Kim, H.M. Park, K.B. Lee, Conformational preference of azaglycine-containing dipeptides studied by PCM and IPCM methods, Chem. Phys. 294 (2003) 201–210.
[29] M.J. Frisch, G.W. Trucks, G.B. Schlegel, P.M.W. Gill, B.G. Johnson, M. A. Robb, J.R. Cheeseman, T. Keith, G.A. Petersson, J.A. Montgomery, K. Raghavachari, M.A.Al-Lagam, V.G. Zakrzewski, J.V. Ortiz, J.B. Foresman, J. Cioslowski, B.B. Stefanov, A. Nanayakkara, M. Challacome, C.Y. Peng, P.Y. Ayala, W. Chen, M.W. Wong, J.L. Anders, E.S. Replogle, R. Gomperts, R.L. Martin, D.J. Fox, J.S. Binkley, D.J. Defrees, J. Baker, J.P. Stewart, M. Head-Gordon, C. Gonzalez, J.A. Pople, Gaussian 94, in: Anonymous, Gaussian, Inc. 1995.
[30] P.A. Karplus, Experimentally observed conformation-dependent geometry and hidden strain in proteins, Protein Sci. 5 (1996) 1406–1420.
[31] H.J. Lee, J.W. Song, Y.S. Choi, H.M. Park, K.B. Lee, A theoretical study of conformational properties of *N*-methyl azapeptide derivatives, J. Am. Chem. Soc. 124 (2002) 11881–11893.
[32] C.H. Reynolds, R.E. Hormann, Theoretical study of the structure and rotational flexibility of diacylhydrazines: implications for the structure of nonsteroidal ecdysone agonists and azapeptides, J. Am. Chem. Soc. 118 (1996) 9395–9401.
[33] H.J. Lee, M.H. Lee, Y.S. Choi, H.M. Park, K.B. Lee, NBO approach to evaluate origin of rotational barrier of diformylhydrazine, J. Mol. Struct., Theochem 631 (2003) 101–110.
[34] O. Farkas, M.A. McAllister, J.H. Ma, A. Perczel, M. Hollosi, I.G. Csizmadia, Peptide models: 19. Side-chain conformational energy surface $E=f$((chi 1, chi 2)) and amide I vibrational frequencies of *N*-formyl-L-phenylalaninamide (For-Phe-NH_2) in its gamma(L) or gamma(inv) or C-7 (eq) backbone conformation, J. Mol. Struct., Theochem 369 (1996) 105–114.
[35] A. Perczel, O. Farkas, A.G. Csaszar, I.G. Csizmadia, Peptide models: 20. Aromatic side-chain–Backbone interaction in phenylalanine-containing diamide model system. A systematic search for the identification of all the ab initio conformers of *N*-formyl-L-phenylalanine-amide, Can. J. Chem. 75 (1997) 1120–1130.
[36] I. Jakli, A. Perczel, O. Farkas, M. Hollosi, I.G. Csizmadia, Peptide models: XXII. A conformational model for aromatic amino acid residues in proteins. A comprehensive analysis of all the RHF/6-31+G conformers of For-L-Phe-NH_2, J. Mol. Struct., Theochem 455 (1998) 303–314.
[37] E.S. Stevens, N. Sugawara, G.M. Bonora, C. Toniolo, Conformational-analysis of linear peptides: 3. Temperature-dependence of NH chemical-shifts in chloroform, J. Am. Chem. Soc. 102 (1980) 7048–7050.